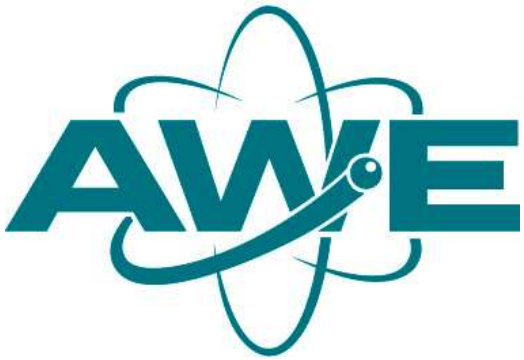

A high order cell centred Lagrangian Godunov scheme for cylindrical geometry

EULAG Workshop

25th-29th June 2012

Andrew Barlow

Introduction (1)

- The staggered grid schemes employed in most hydrocodes have been remarkably successful.
- However, they clearly have some theoretical and practical deficiencies.
- Mesh imprinting and symmetry breaking are important examples.
- The need to use artificial viscosities, hourglass filters and subzonal pressure schemes is undesirable.
- A staggered mesh is also inelegant in that all variables are not conserved over the same space.
- High resolution cell centred Lagrangian Godunov schemes could overcome some of these problems.

Introduction (2)

- However, while Eulerian Godunov methods have been well established for a long time [Godunov (MS, 1959)] progress has been slow in extending these ideas to Lagrangian and ALE schemes.
- This has largely been due to the difficulty in defining consistent Lagrangian nodal velocities with which to move the computational mesh.
  - CAVEAT scheme [Dukowicz et al. (LANL report, 1986)]
- However, significant progress has been made recently in solving this problem:
  - 3rd DG scheme [Loubere et al. (IJNF, 2004)]
  - GLACE scheme [Despres and Manzeran (ARMA, 2005)]
  - EUCCLYHD scheme [Maire et al. (SISC, 2007)]
  - Burton and Shashkov [Multimat presentations]

Introduction (3)

- Most Lagrangian Godunov schemes either define nodal velocities as an average of adjacent cell centred or edge velocities (from the Riemann solver), or introduce a special nodal Riemann solver.
- An alternative dual grid approach has also been developed by the author. This talk will discuss the extension of the 1st order scheme described in [1] to 2nd order in space and time, the extension of the scheme to cylindrical geometry and preliminary results from extension of the scheme to include an elastoplastic flow capability.

---

[1] Barlow AJ, Roe PL, 'A cell centred Lagrangian Godunov scheme for shock hydrodynamics'. Comput. Fluids., **46,** issue1, (2011), 133-136.

Transient dual grid idea

- All variables conserved at element centres.
- **Nodal velocities are either reconstructed at start of time step or carried as an additional variable.**
- Acceleration of nodes during the time step is calculated by solving an additional momentum equation on transient dual grid.
- The finite volume update of the conserved element centred variables is performed using fluxing volumes that are consistent with the motion of the nodes.

Construction of nodal velocities

- An acoustic approximate Riemann solver is used to define the normal velocity v* on each cell edge

$$v_a^* = \frac{\rho_{1a}c_{1a}u_{1a} + \rho_{2a}c_{2a}u_{2a} + p_{1a} - p_{2a}}{\rho_{1a}c_{1a} + \rho_{2a}c_{2a}}$$

- A system of equations is then solved to determine a corner velocity $\mathbf{u}_c$ which match v* on the two adjacent edges a and b

$$v_a^* = \hat{n}_a \cdot \vec{u}_c \qquad v_b^* = \hat{n}_b \cdot \vec{u}_c$$

- The nodal velocity is then obtained by averaging all the corner velocities associated with the node

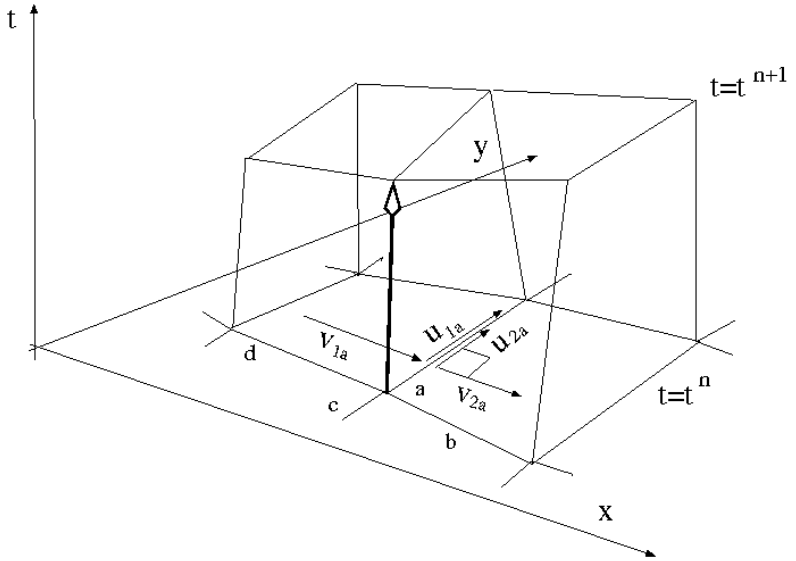

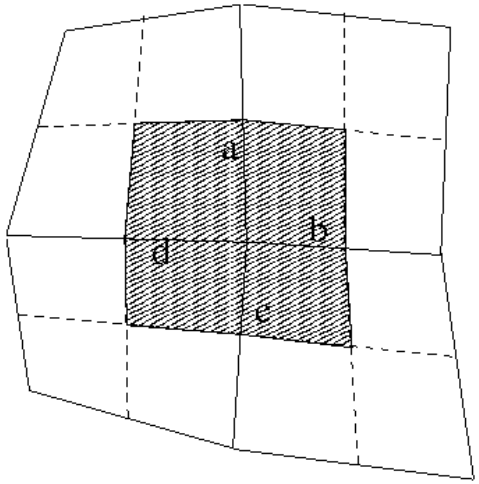

Nodal acceleration calculation

- P* is required on each of the internal dual grid boundaries in order to solve the nodal momentum equation

$$M_D\left(\frac{d\bar{u}_C}{dt}\right)^{n+\frac{1}{2}} = -\int_{\partial D}\left(p^*\right)^{n+\frac{1}{2}} d\vec{n}$$

- The P* for each median mesh line is obtained by solving a collision Riemann problem using the zonal state variables and the nodal velocities reconstructed at the start of the time step.

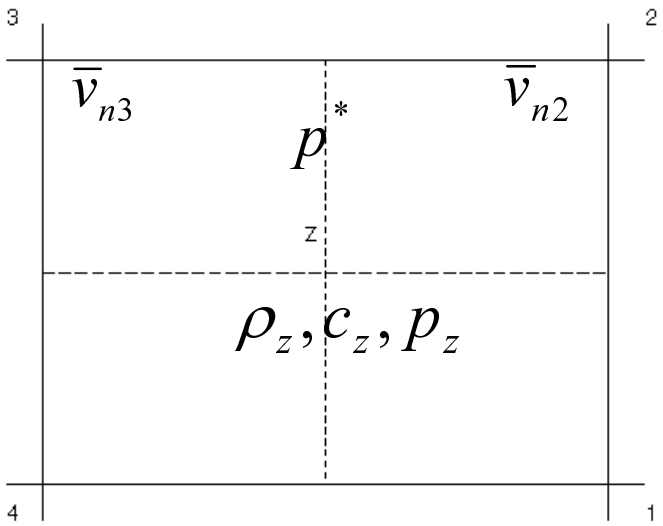

Approximate Riemann Solver (1)

- Artificial viscosity methods are often designed to only act normal to the shock front or in the direction of the velocity jump.
- The same idea has been applied here to the acoustic approximate Riemann solver to make it into a simple multi-dimensional solver

$$p^* = \frac{z_{1a}p_{2a} + z_{2a}p_{1a}}{z_{1a} + z_{2a}} \qquad \bar{q}^* = \frac{z_{1a}z_{2a}(\bar{v}_{2a} - \bar{v}_{1a})}{z_{1a} + z_{2a}}$$

where

$$z_{1a} = \rho_{1a}(c_{1a} + \Gamma \mid v_{2a} - v_{1a} \mid)$$

- This effectively introduces linear and quadratic artificial viscosity like terms as suggested by Dukowicz.

Approximate Riemann Solver (2)

- The zonal and nodal momentum equations can now be written as

$$M_{z,D}\left(\frac{d\bar{u}_{z,D}}{dt}\right)^{n+\frac{1}{2}} = -\int_{\partial D,Z}\left(p^*\right)^{n+\frac{1}{2}}d\vec{n} - \int_{\partial D,Z}\bar{q}^{\,*}\,ds$$

- The right hand side of these equations can now be viewed as the gathering of forces that are acting on a zone or node.
- From this analogy it is clear how to modify the total energy update to allow for the new approximate Riemann solver.

$$M_z\left(\frac{dE_z}{dt}\right)^{n+\frac{1}{2}} = -\int_{\partial Z}\left(p^*\right)^{n+\frac{1}{2}}\bar{u}\;\;.d\vec{n} - \int_{\partial Z}\left(\bar{q}\right)^{n+\frac{1}{2}}\cdot\bar{u}^{\,n+\frac{1}{2}}ds$$

where u_e is the average velocity of the two nodes defining edge e.

Time Discretization (1)

Optional – Nodal velocity reconstruction – requires solution of Riemann problem for v* at cell boundaries

$$x^{n+\frac{1}{2}} = x^{n} + \frac{1}{2}u^{n}\Delta t \forall nodes$$

$$V^{n+\frac{1}{2}} = V\left(x^{n+\frac{1}{2}}\right)\forall cells$$

$$\rho^{n+\frac{1}{2}} = \frac{M^{e}}{V^{n+\frac{1}{2}}}$$

Solve Riemann problem for P^{n*}

$$M_z \frac{dE_z^{n+\frac{1}{2}}}{dt} = -\int_{s_k} (p_e^{n*}\bar{u}_e^{n}.\bar{n}_e^{n} + \bar{q}_e^{n*}\cdot\bar{u}_e^{n})dA$$

Define edge velocity u_e as average velocity of two nodes defining edge

Predictor total energy update

$$P^{n+\frac{1}{2}} = P\left(\varepsilon^{n+\frac{1}{2}}, \rho^{n+\frac{1}{2}}\right)$$

Equation of State call

$$\varepsilon_z^{n+\frac{1}{2}} = E_z^{n+\frac{1}{2}} - \frac{1}{2}\| u_z^{n} \|^2$$

Time Discretization (2)

Solve Riemann problem for $P^{n+1/2*}$ at cell boundaries

$$M_z \frac{d\bar{u}_z^{n+1}}{dt} = -\int_{s_k} (p_e^{n+\frac{1}{2}*} \bar{n}_e^{n+\frac{1}{2}*} + \bar{q}_e^{n+\frac{1}{2}*}) dA$$ **Zonal accelerations**

Acceleration calculation - centred pressure for 2nd order accuracy in time

Solve Riemann problem for $P^{n+1/2*}$ at dual mesh boundaries

$$M_p \frac{d\bar{u}_p^{n+1}}{dt} = -\int_{s_k} (p_d^{n+\frac{1}{2}*} \bar{n}_d^{n+\frac{1}{2}*} + \bar{q}_d^{n+\frac{1}{2}*}) dA$$ **Nodal accelerations**

where $\bar{u} = \frac{1}{2}\left(u^n + u^{n+1}\right)$

$$x^{n+1} = x^n + \bar{u}\Delta t \forall nodes$$

$$\rho^{n+1} = \frac{M^e}{V^{n+1}}$$

$$V^{n+1} = V(x^{n+1}) \forall cells$$

$$M_z \frac{dE_z^{n+1}}{dt} = -\int_{s_k} (p_e^{n+\frac{1}{2}*} \bar{u}_e^{n+\frac{1}{2}} . \bar{n}_e^{n+\frac{1}{2}} + \bar{q}_e^{n+\frac{1}{2}*} \cdot \bar{u}_e^{n+\frac{1}{2}}) dA$$

Corrector total energy update

Define edge velocity u_e as average velocity of two nodes defining edge

$$P^{n+1} = P(\varepsilon^{n+1}, \rho^{n+1})$$ **Equation of State call**

$$\varepsilon_z^{n+1} = E_z^{n+1} - \frac{1}{2} || u_z^{n+1} ||^2$$

2nd order extension (1)

- Slope extrapolation is used to determine the velocities and pressures at the cell edges, when the a solution to the Riemann problem is required across cell edges.
- Three slopes are calculated in volume coordinates in each isoparametric direction.

$$\frac{\partial \phi_\alpha}{\partial x} = \frac{(\phi_{\alpha+1} - \phi_\alpha)\Delta x_\alpha^2 + (\phi_\alpha - \phi_{\alpha-1})\Delta x_{\alpha+1}^2}{\Delta x_\alpha \Delta x_{\alpha+1}(\Delta x_\alpha + \Delta x_{\alpha+1})}$$

$$\Delta\phi_{\alpha+1} = \frac{\phi_{\alpha+1} - \phi_\alpha}{\Delta x_{\alpha+1}} \qquad \Delta\phi_\alpha = \frac{\phi_\alpha - \phi_{\alpha-1}}{\Delta x_\alpha}$$

2nd order extension (2)

- A van Leer slope limiter is then use to define the slope use for the extrapolation

$$\phi'_{\alpha} = \frac{1}{2}\left(\mathrm{sgn}\left(\Delta\phi_{\alpha}\right)+\mathrm{sgn}\left(\Delta\phi_{\alpha+1}\right)\right)\min\left(\left|\frac{\partial\phi_{\alpha}}{\partial x}\right|,\left|\Delta\phi_{\alpha}\right|,\left|\Delta\phi_{\alpha+1}\right|\right)$$

- A second order approach is not used for the nodal quantities on the dual grid when solving the nodal momentum equation to move the nodes as little sensitivity has been observed as to whether a first or second order method is used for the nodal momentum solve.

Sod's Shock tube

- 100 zones. Ideal gas (γ=1.4). State variables (p, ρ, ε) = (1.0, 0.125, 2.5)$_L$ and (0.1, 0.1, 2.0)$_R$.

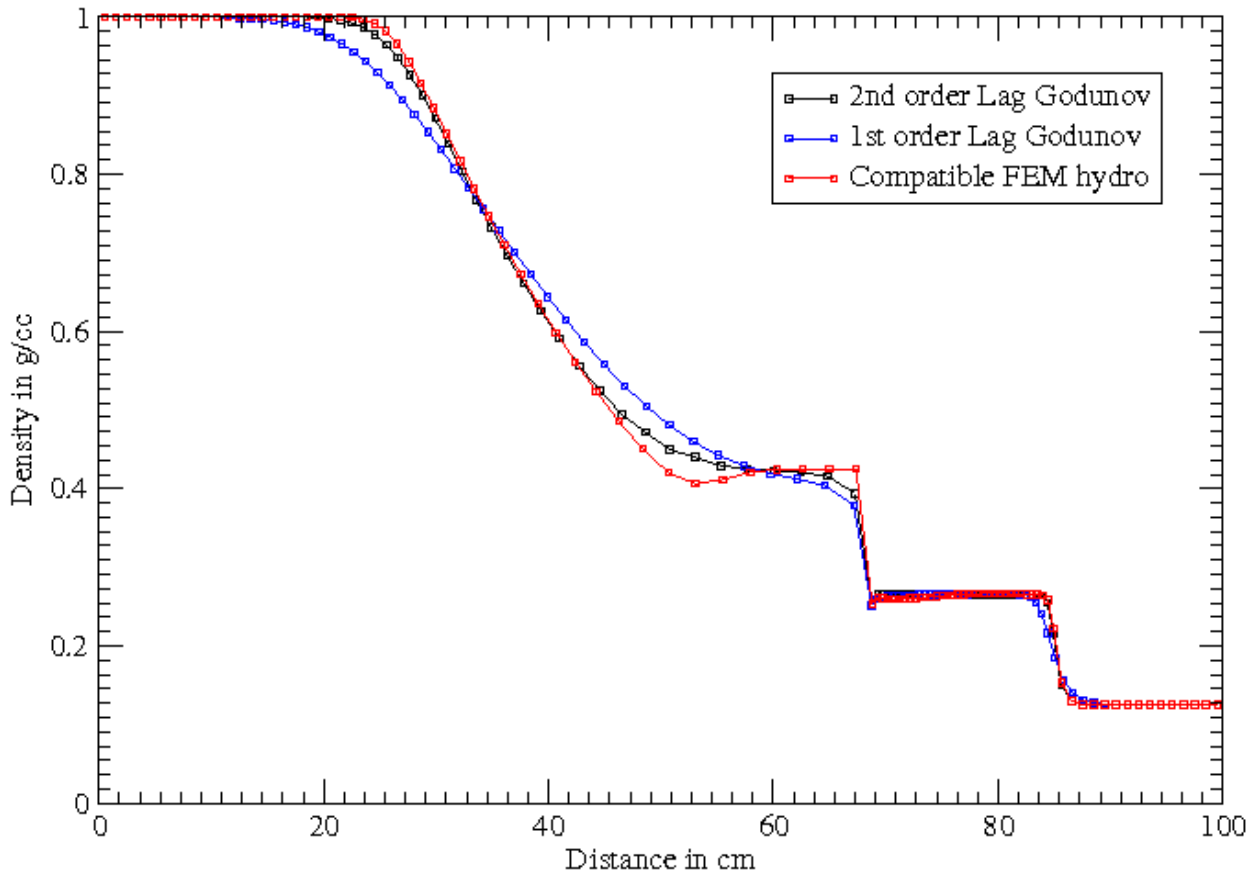

Saltzman's Piston Problem (1)

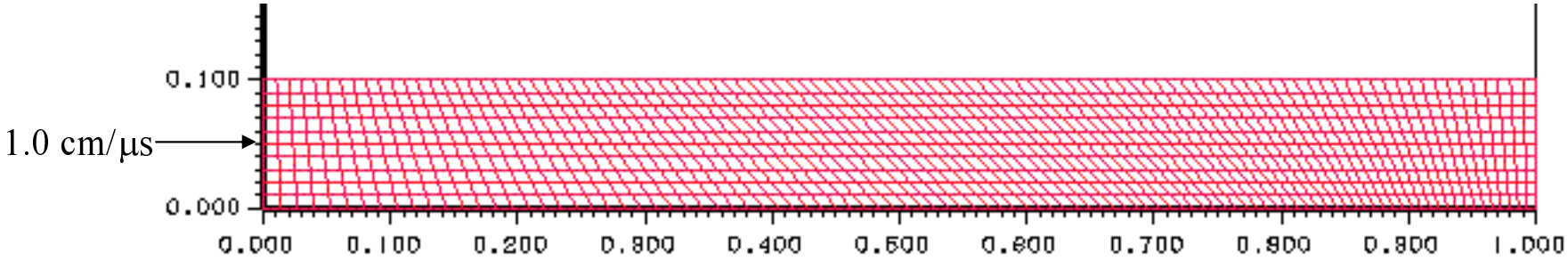

- Piston moves with unit velocity from left to right generating a shock that passes across a grid that is skewed with respect to the vertical with a half sin wave perturbation. The right end is treated as a reflecting boundary.
- Ideal gas (γ=1.66) with unity initial density and zero internal energy.
- Compare mesh quality and density behind before and after reflection.
- A density of 4 g/cc should be observed behind first shock and 10 g/cc behind reflected shock.

Saltzman's Piston Plane Geometry (2)

2nd order Godunov **with** reconstruction

t=0.7 μs

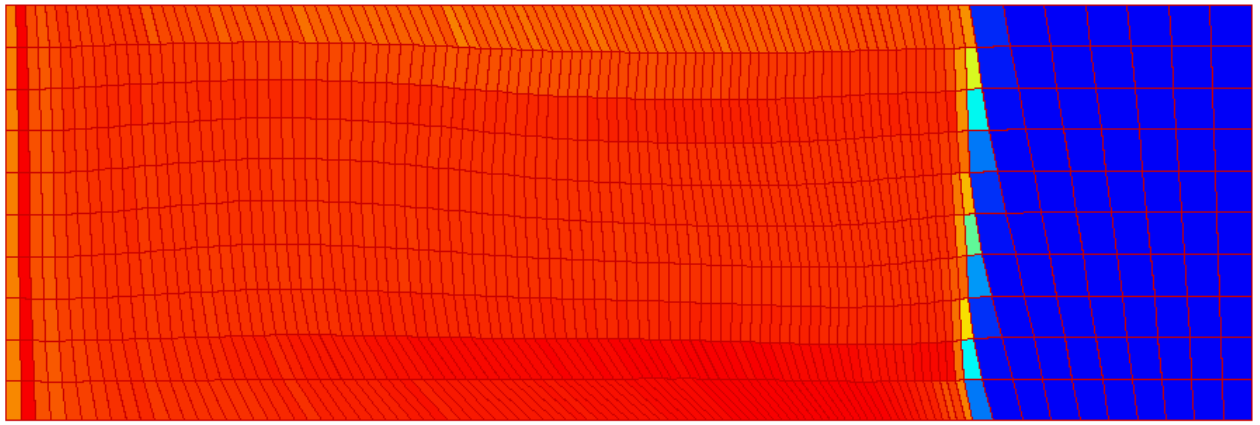

2nd order Godunov **without** reconstruction

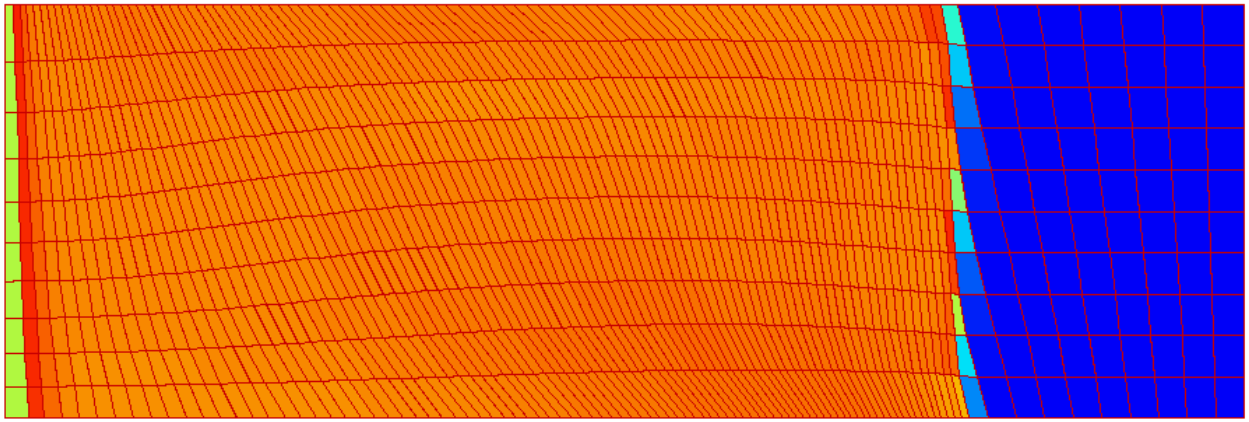

Initial angle of mesh lines not preserved by reconstruction!

Saltzman's Piston Plane Geometry (3)

2nd order Godunov **with** reconstruction

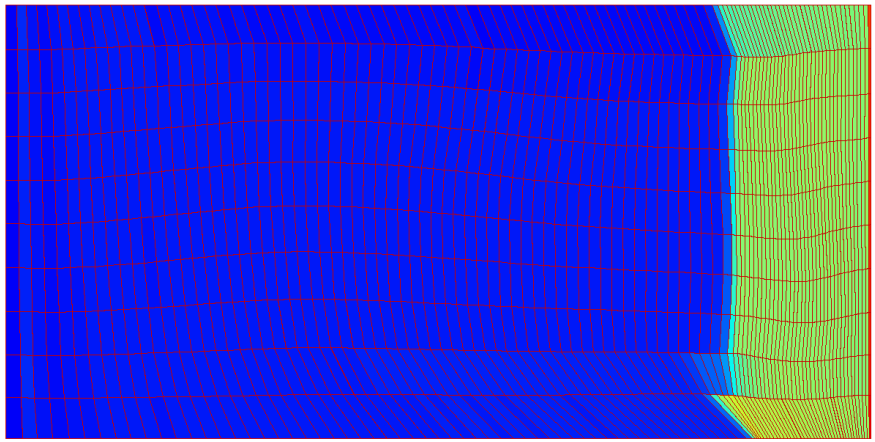

t=0.8 μs

2nd order Godunov **without** reconstruction

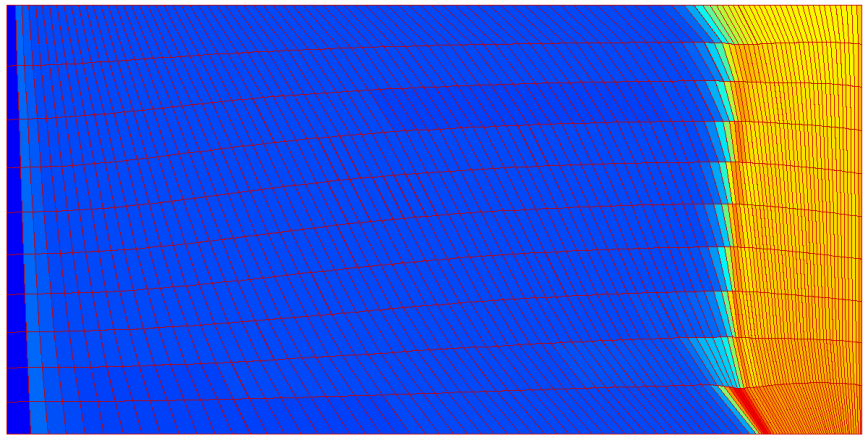

Initial angle of mesh lines not preserved by reconstruction!
Reconstruction method appears to introduce additional dissipation.

Saltzman's Piston Plane Geometry (4)

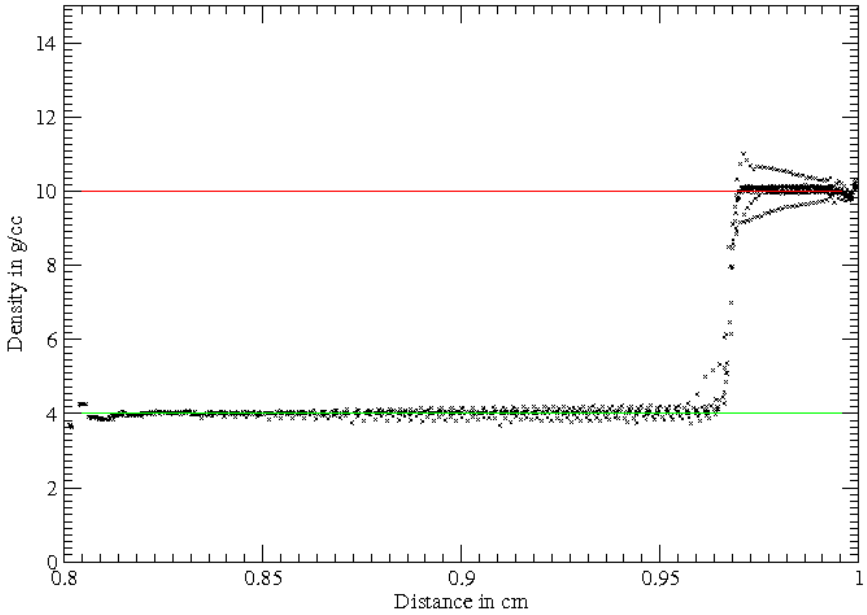

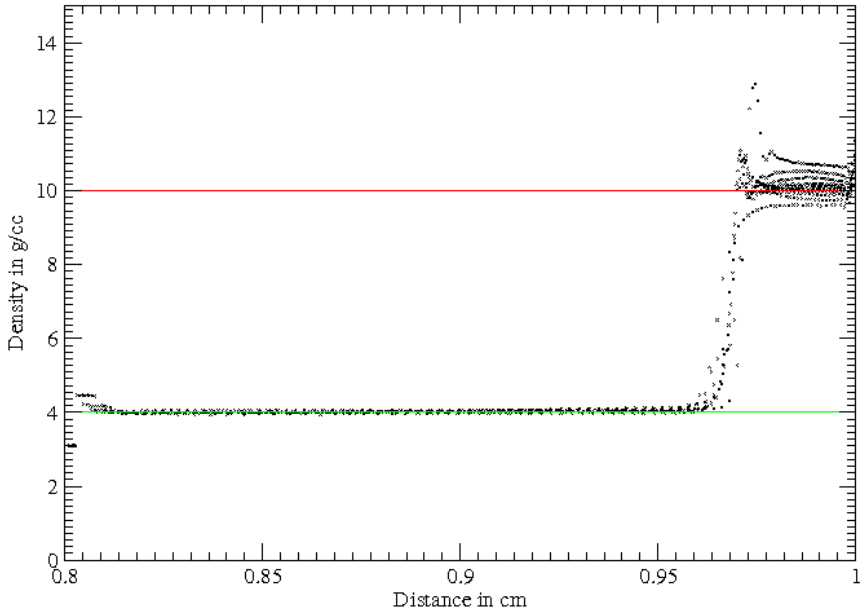

2nd order Godunov **with** reconstruction

T=0.8 μs

2nd order Godunov **without** reconstruction

Density more uniform behind first shock without reconstruction,
but more of an overshoot for reflected shock and more smearing of shock front.
Local error in shock position at boundary apparent in both solutions.

Noh Problem

- Plane geometry with R θ and X Y mesh variants considered.
- Ideal gas (γ=1.66) with unity initial density and zero internal energy.
- Initial uniform radial velocity imposed acting towards the origin.

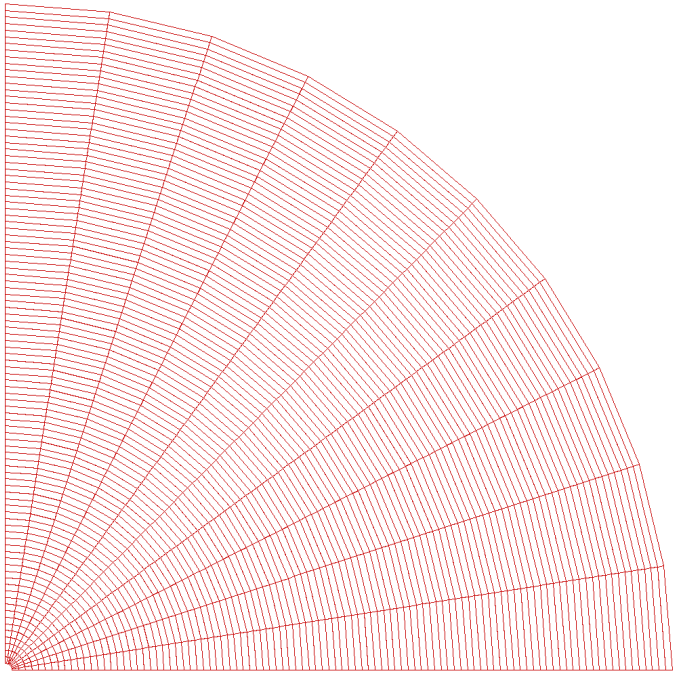

Initial meshes

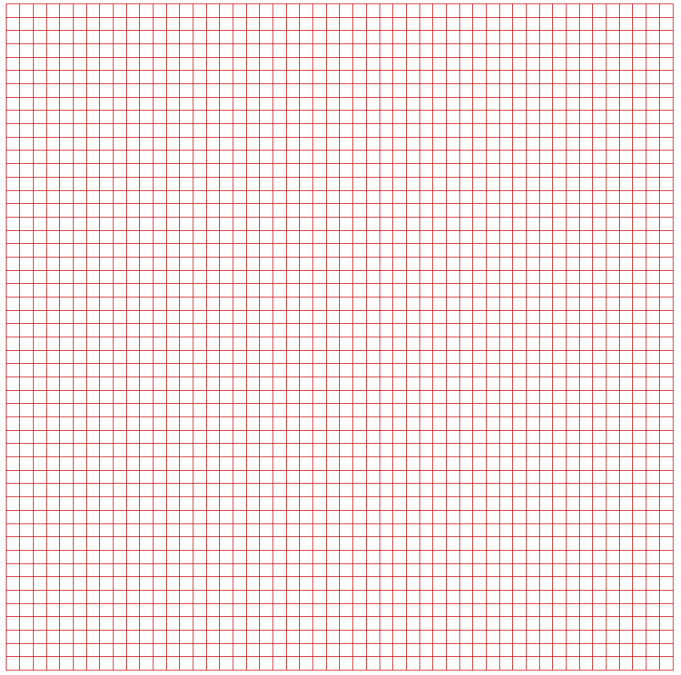

Noh in Plane Geometry (1)

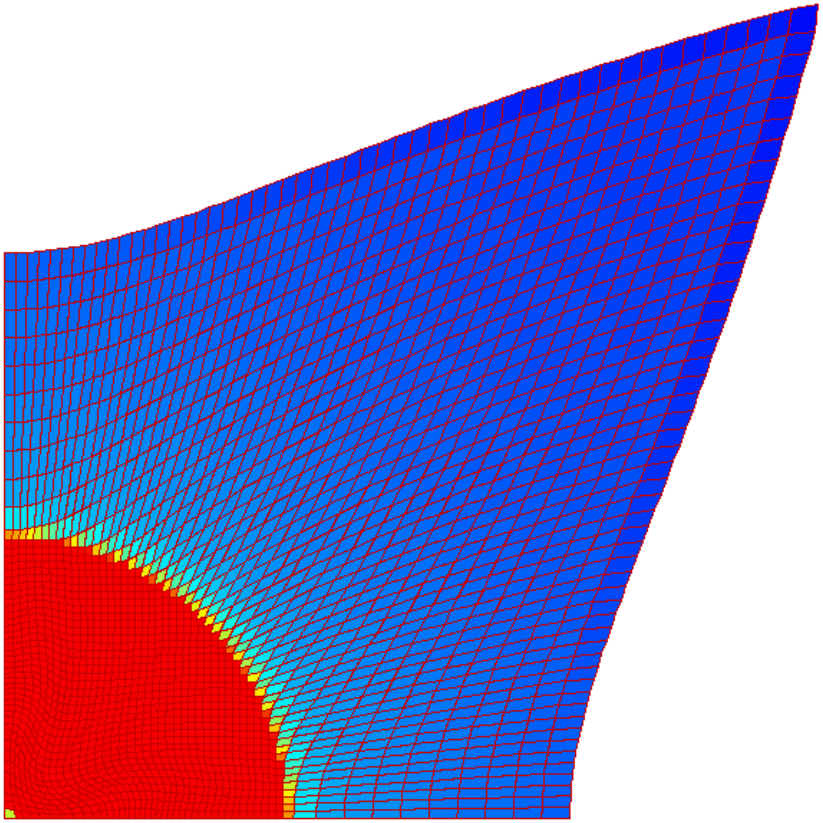

2nd order Godunov **with** reconstruction

T=0.6 μs

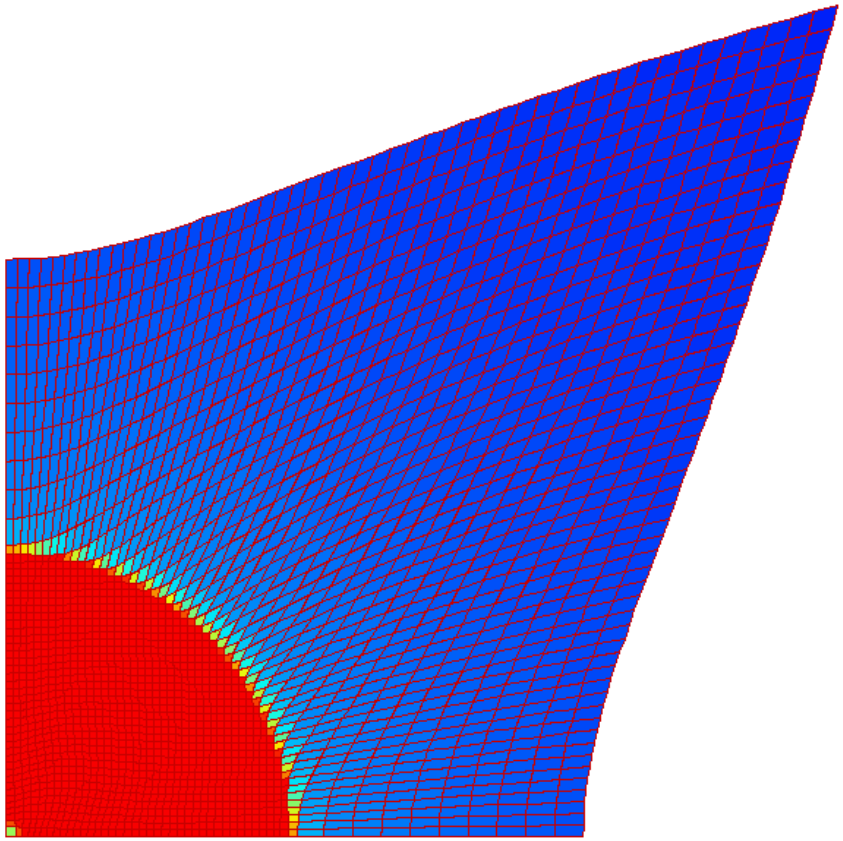

2nd order Godunov **without** reconstruction

Noh in Plane Geometry (2)

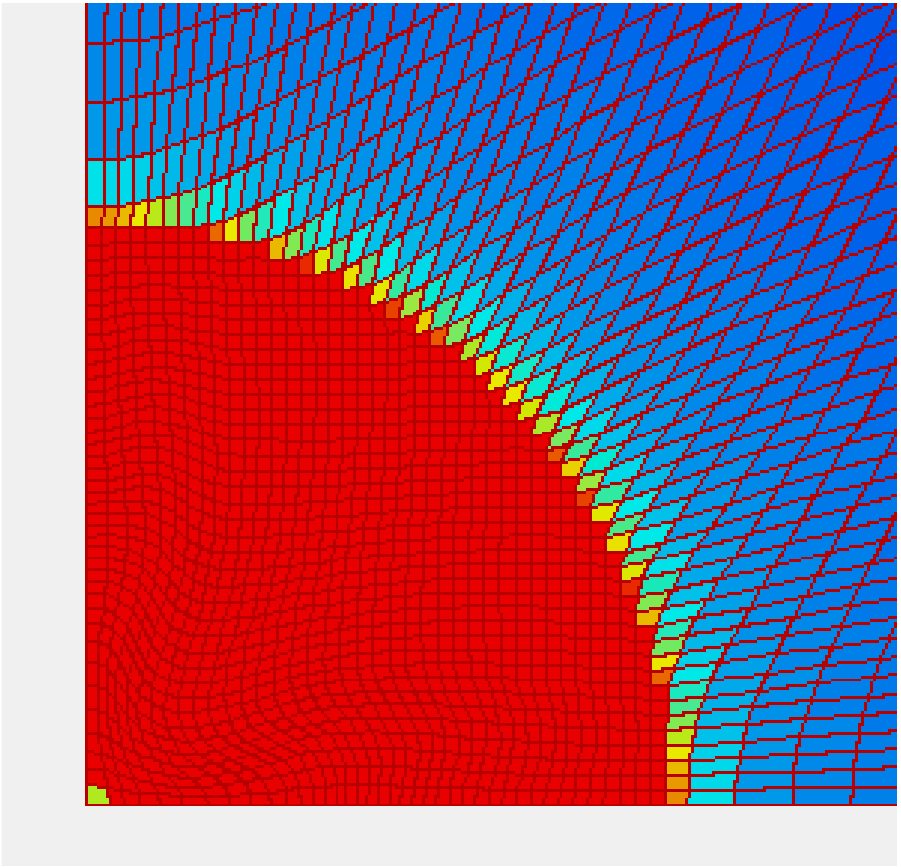

2nd order Godunov **with** reconstruction

T=0.6 μs

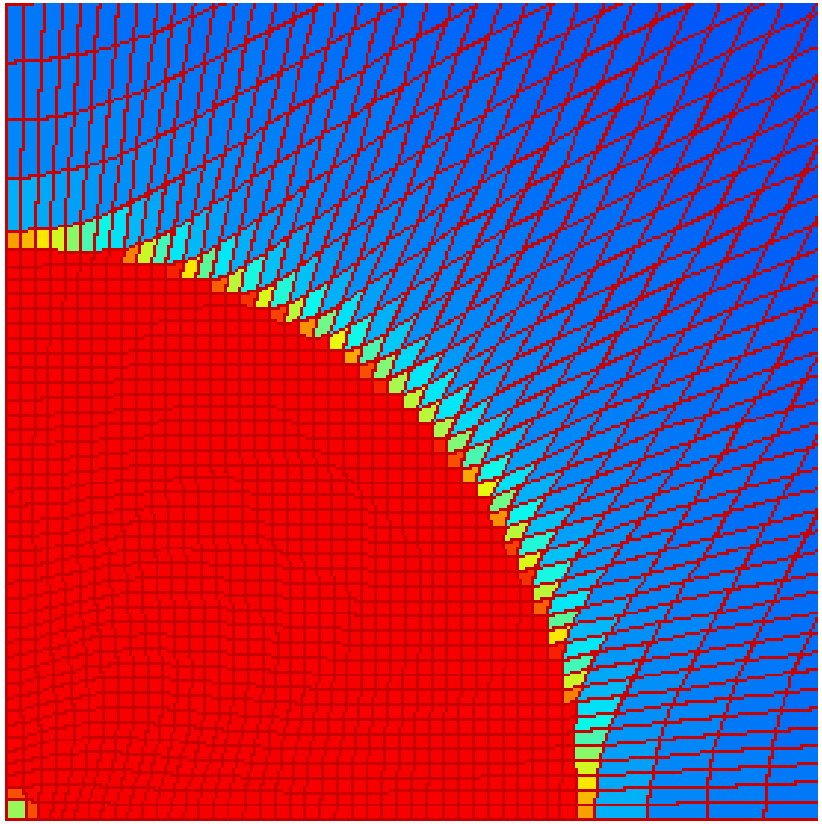

2nd order Godunov **without** reconstruction

Noh in Plane Geometry - Density (3)

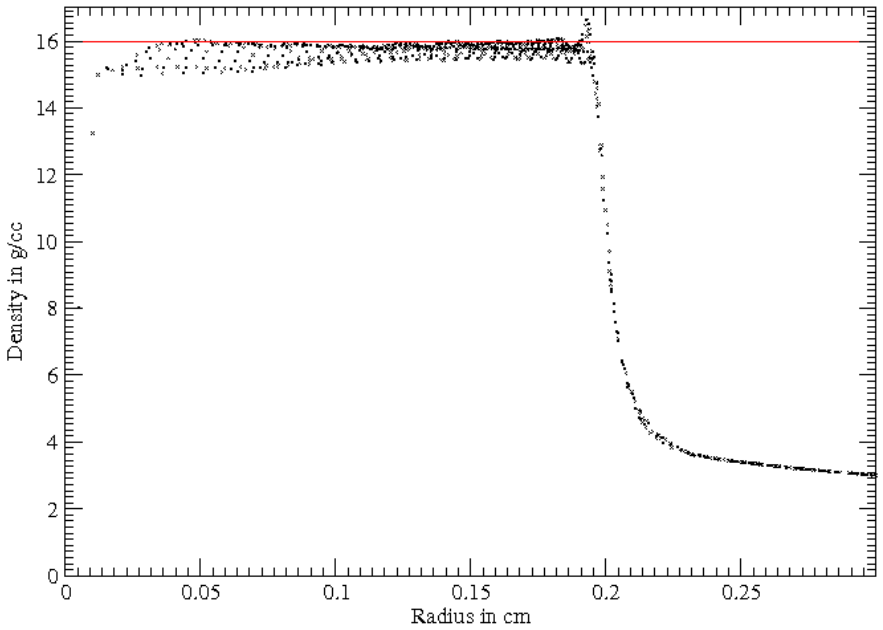

2nd order Godunov **with** reconstruction

T=0.6 μs

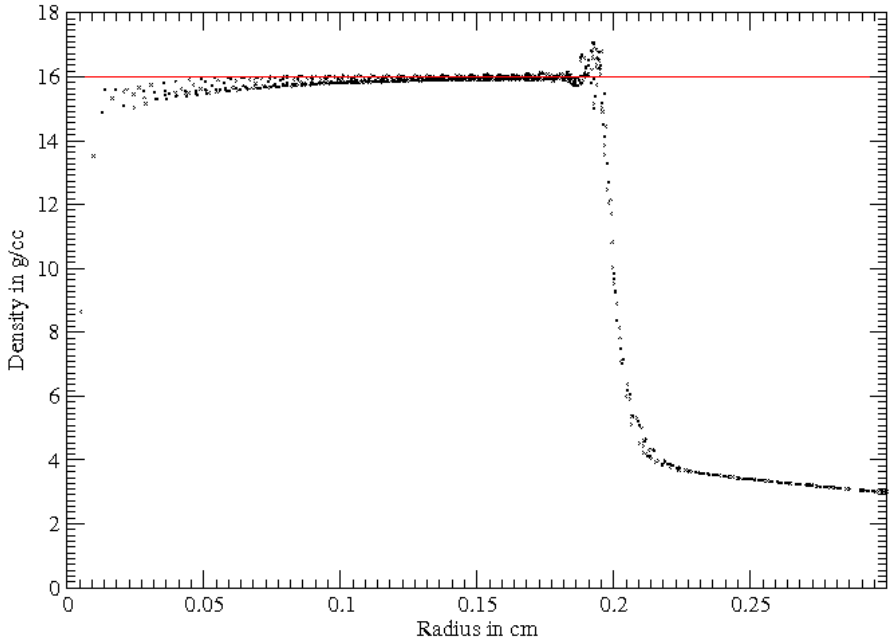

2nd order Godunov **without** reconstruction

Density is more uniform behind outgoing shock, mesh quality and symmetry are improved and shock smearing is reduced without reconstruction, but a larger overshoot is observed at the shock front.

Cylindrical Geometry

- An area weighted approach has been taken to extend the method to cylindrical geometry.
- This effectively solves the two momentum equations as for plane geometry case.
- The total energy update is modified to account for the true swept volume associated with each edge in cylindrical geometry by simply using the expression for the average face centred velocity weighted by radius suggested by Pierre-Henri Maire [2]:

$$R_f^c \overline{U}_f^c = \frac{1}{2}\left(\frac{2R_p + R_{p+}}{3}\overline{U}_p + \frac{R_p + 2R_{p+}}{3}\overline{U}_{p+} \right)$$

[2] Maire, P-H, 'A high-order cell centred Lagrangian Godunov scheme for compressible fluid flows in two-dimensional cylindrical geometry', Journal of Computational Physics, 228, (2009), 6882-6915.

Saltzman's Piston in Cylindrical Geometry (2)

Compatible FEM hydro in cylindrical geometry

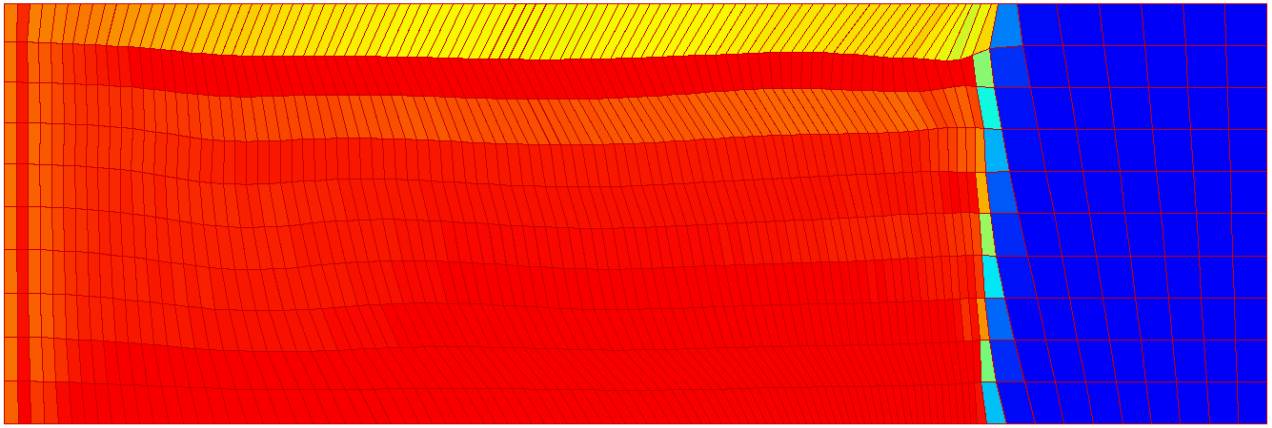

t=0.7 μs

2nd order Godunov **without** reconstruction in cylindrical geometry

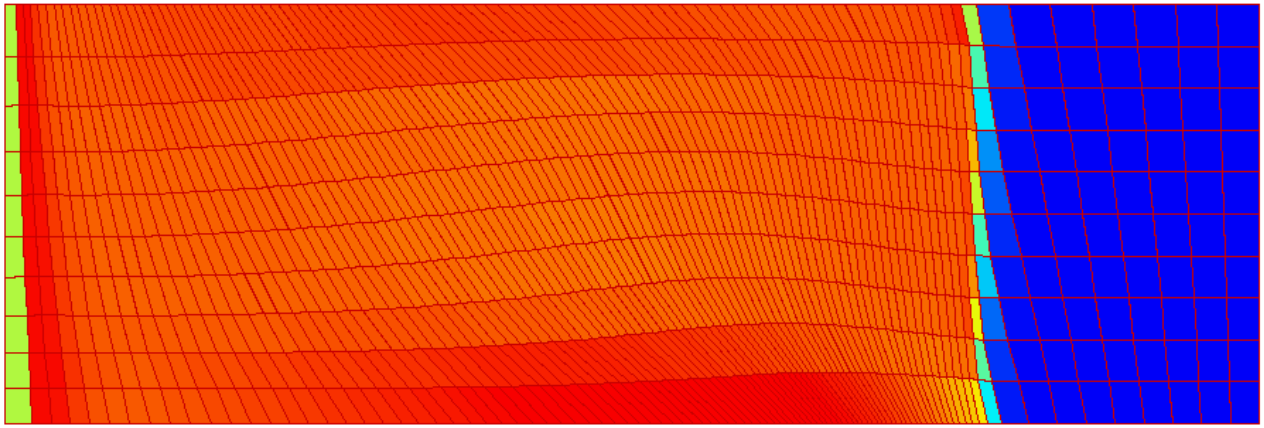

Saltzman's Piston in Cylindrical Geometry (3)

Compatible
FEM hydro in
cylindrical geometry

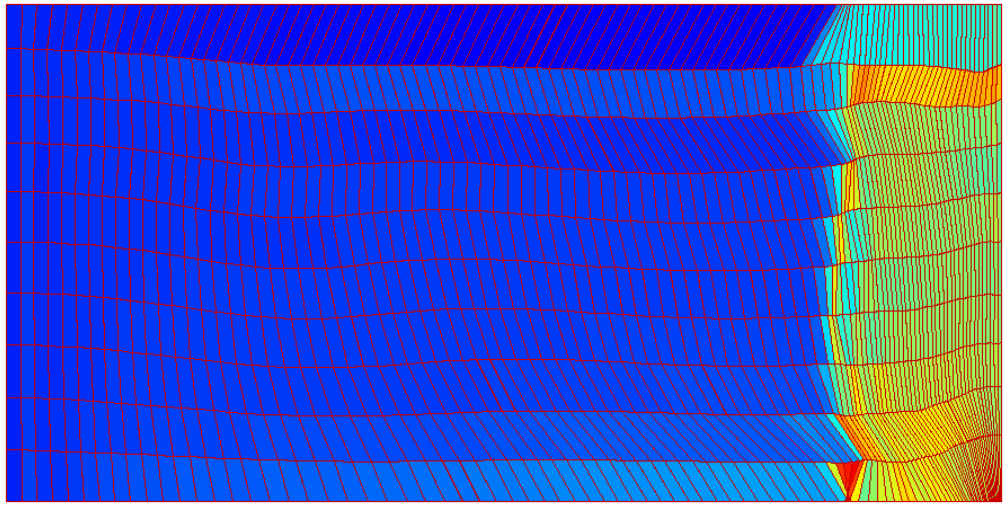

t=0.8 μs

2nd order
Godunov **without**
reconstruction in
cylindrical geometry

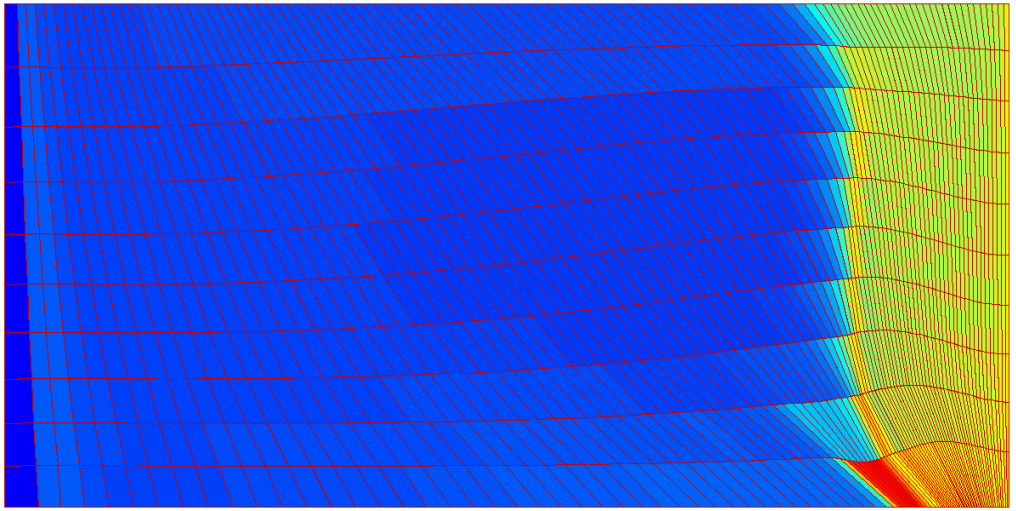

Saltzman's Piston in Cylindrical Geometry (4)

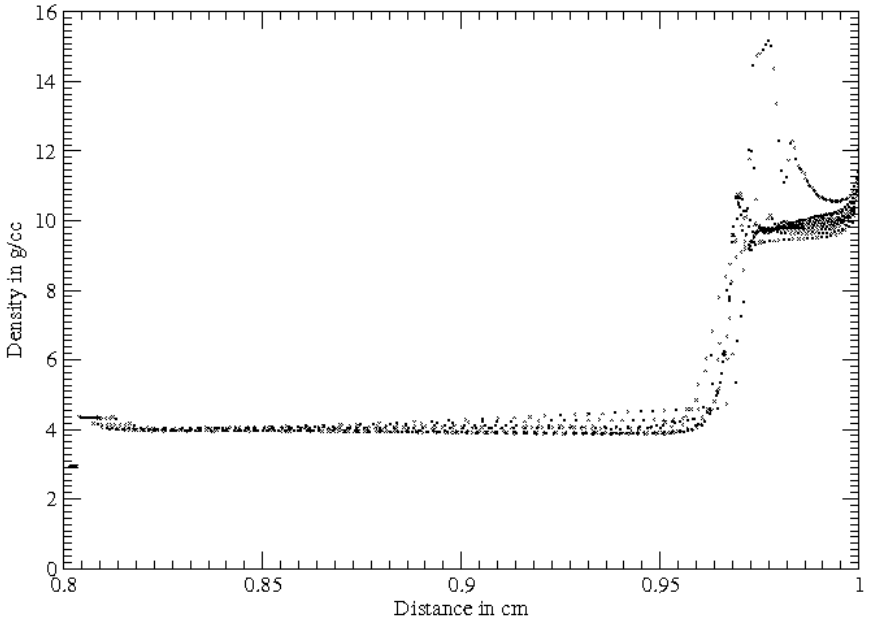

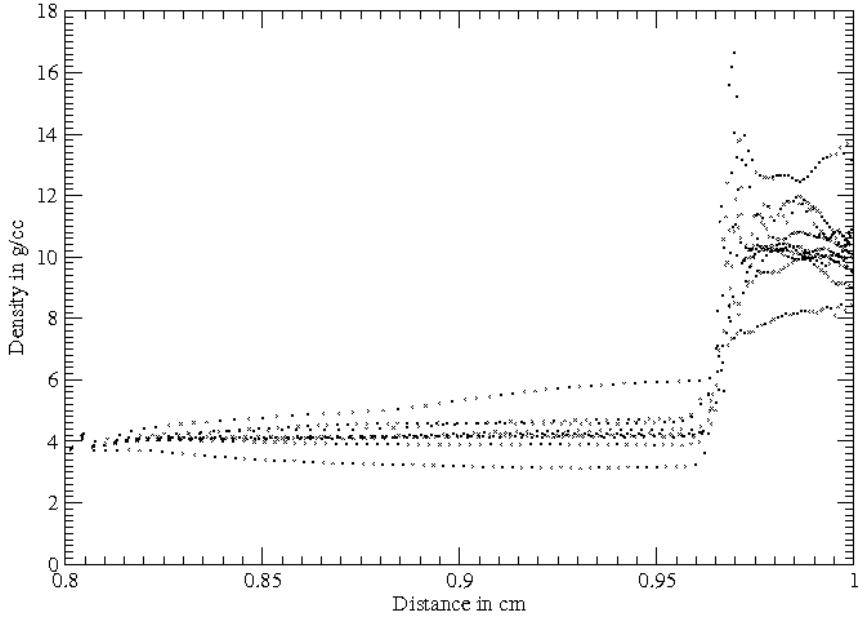

2nd order Godunov **without** reconstruction in cylindrical geometry

T=0.8 μs

Compatible FEM hydro in cylindrical geometry

Noh in Cylindrical Geometry on R Theta grid

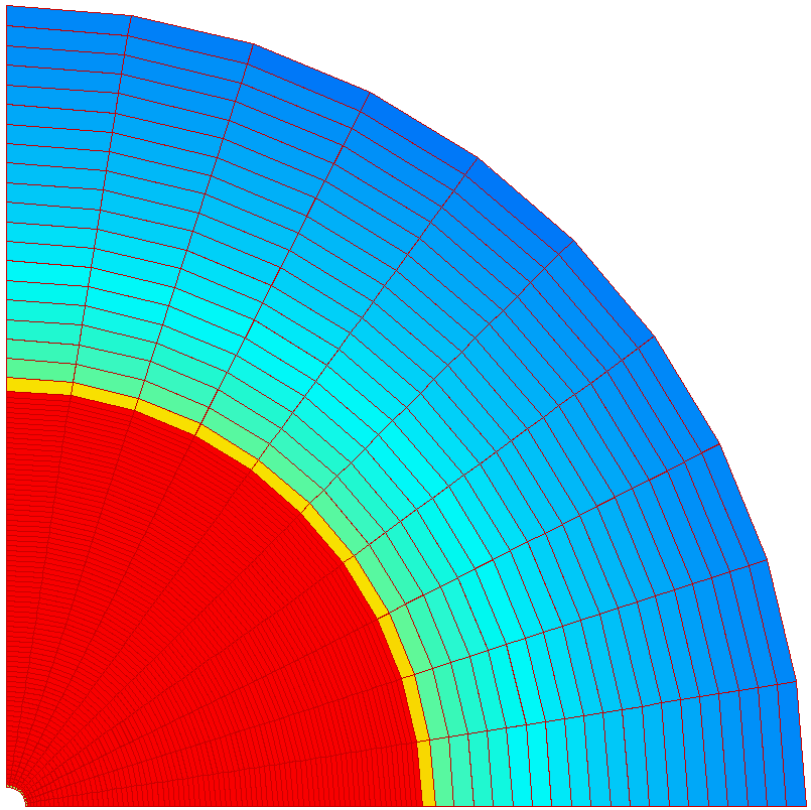

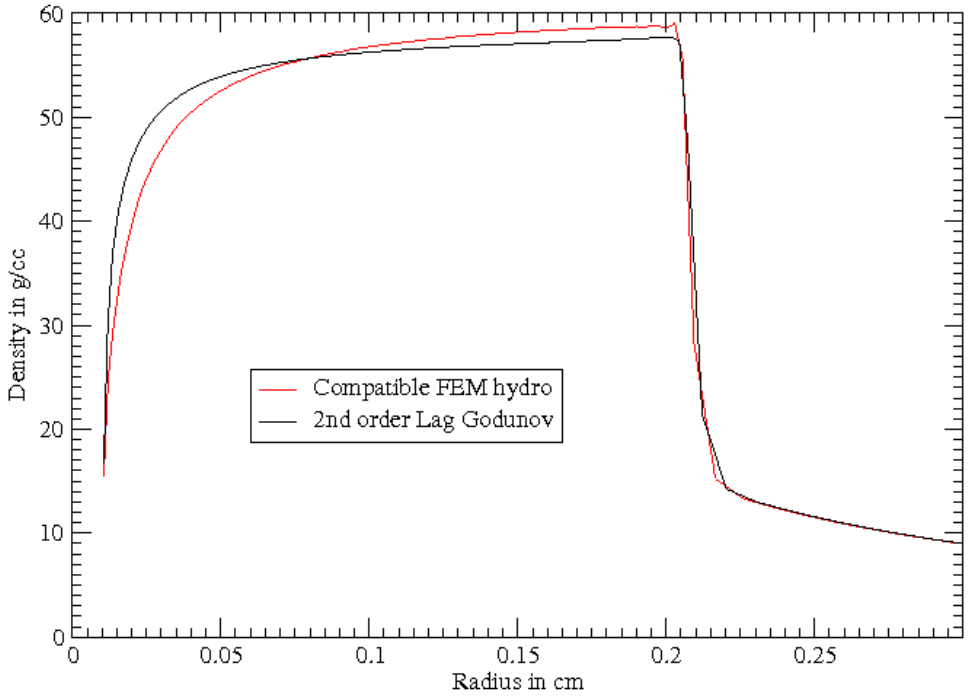

2nd order Godunov
without reconstruction
in cylindrical geometry

T=0.6 μs

Density profile comparison

Noh in cylindrical geometry on initially cartesian grid (1)

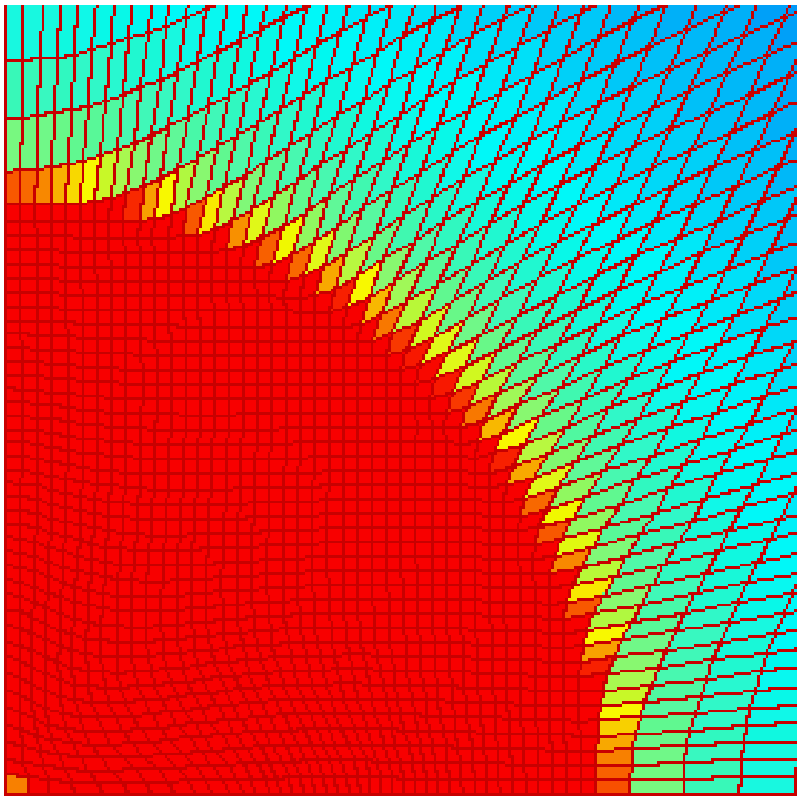

2nd order Godunov without reconstruction in cylindrical geometry

T=0.6 μs

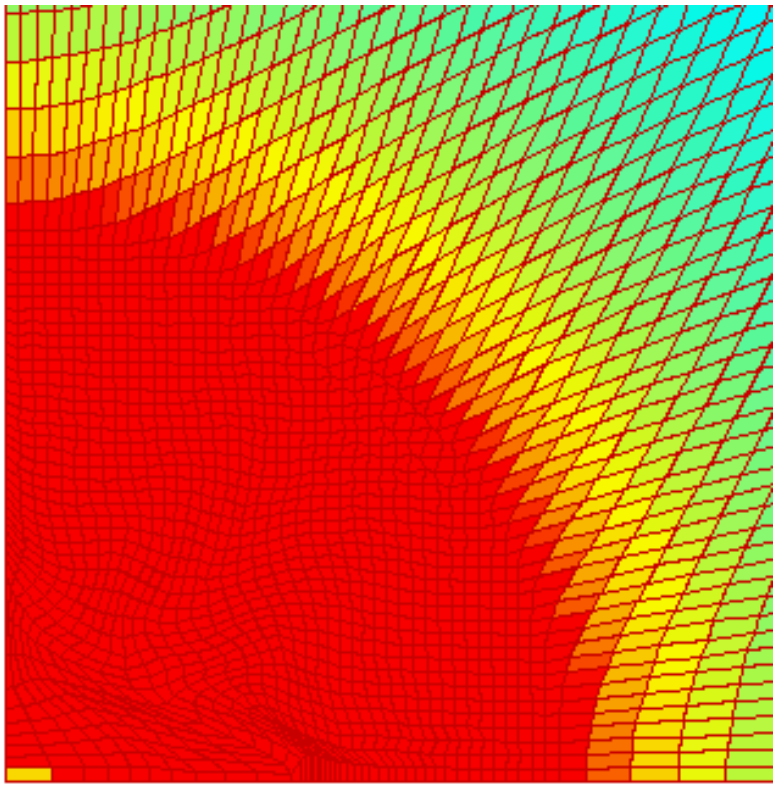

Compatible FEM hydro in cylindrical geometry

Noh in cylindrical geometry on initially cartesian grid (2)

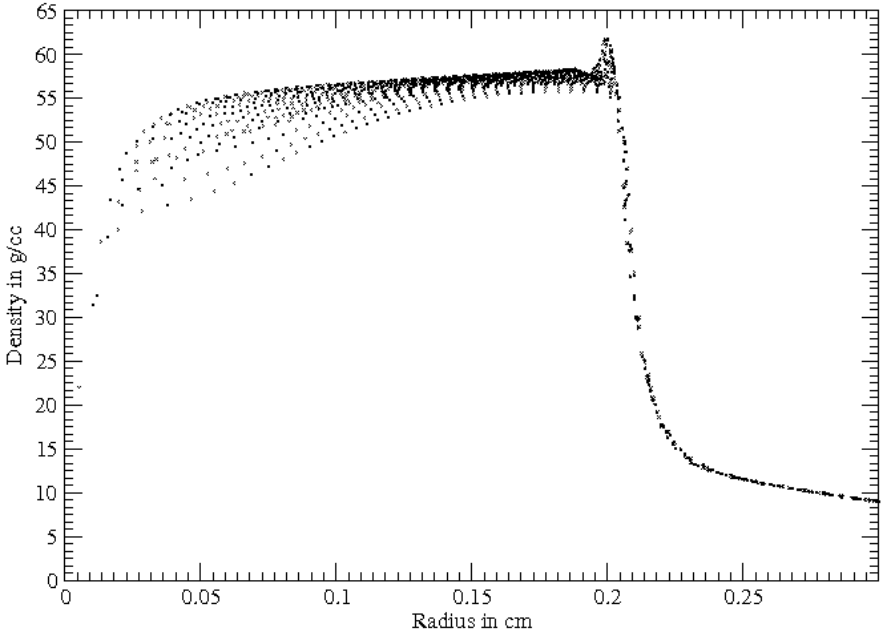

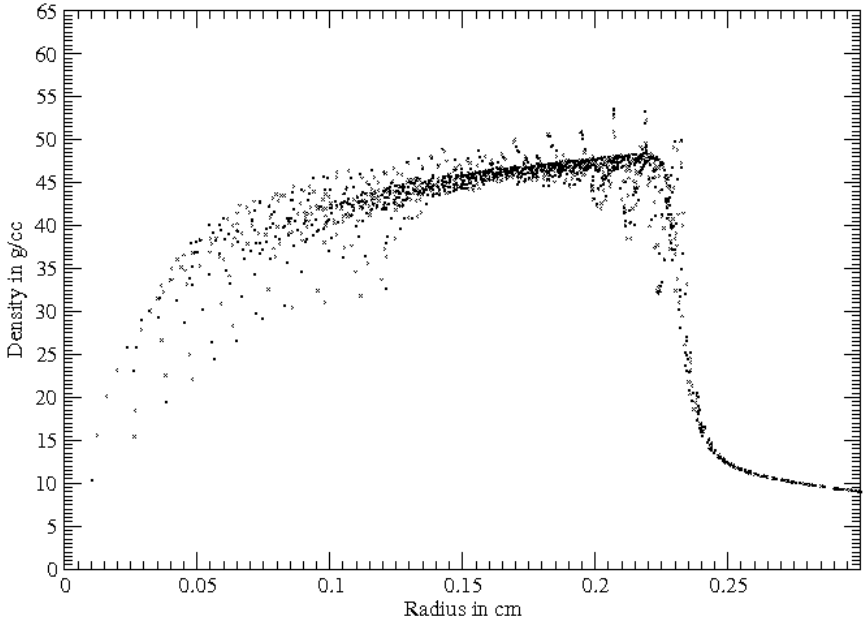

T=0.6 μs

2nd order Godunov **without** reconstruction in cylindrical geometry

Compatible FEM hydro in cylindrical geometry

Sedov in cylindrical geometry (1)

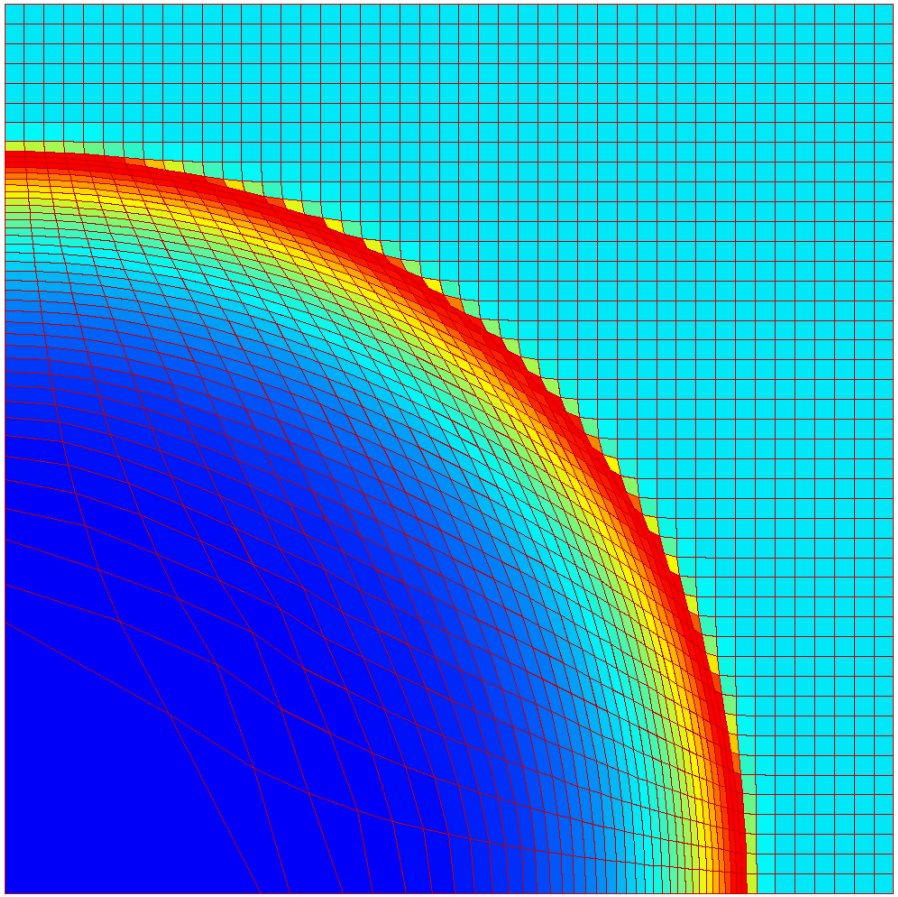

2nd order Godunov
without reconstruction
in cylindrical geometry

T=1.0 μs

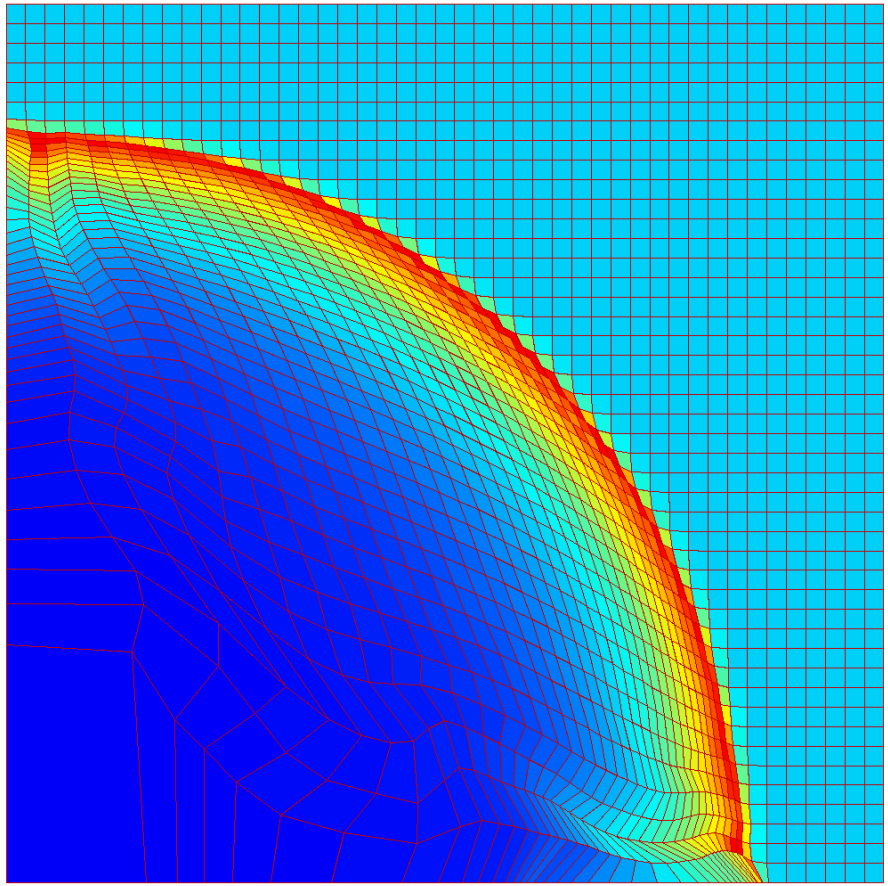

Compatible FEM hydro in
cylindrical geometry

Sedov in cylindrical geometry (2)

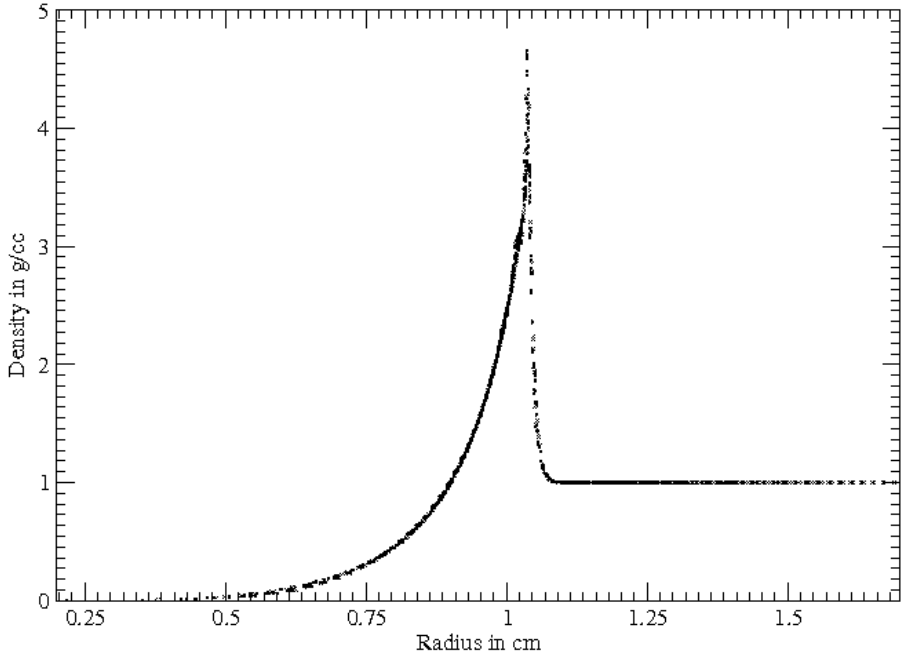

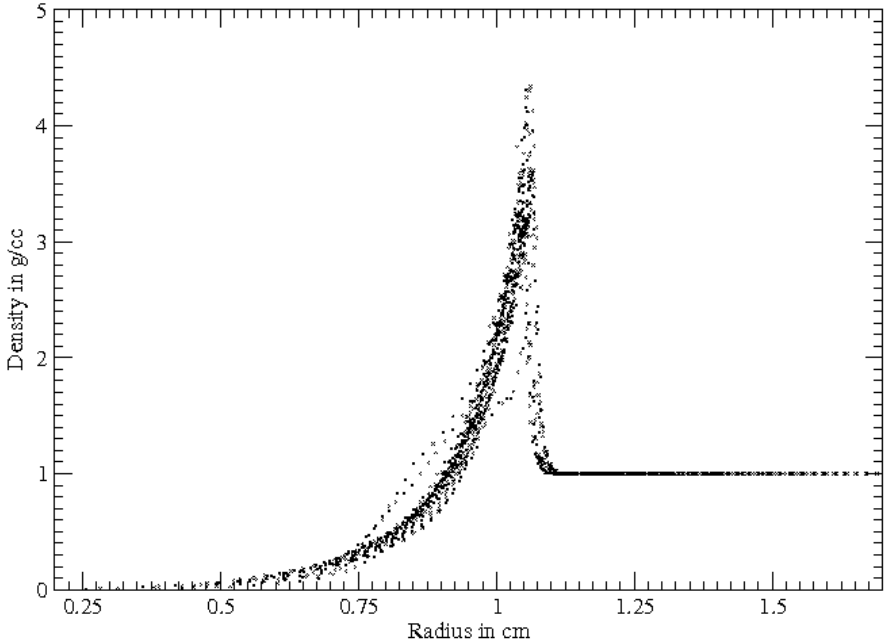

T=1.0 μs

2nd order Godunov **without** reconstruction in cylindrical geometry

Compatible FEM hydro in cylindrical geometry

Elastoplatic flow capability (1)

- Force terms in momentum and total energy equations extended to include stress deviators.
- Nodal velocities used to calculate strain rates at element centres.
- Stress deviators at element centres obtained following standard staggered grid method (Wilkins).
- Slope extrapolation used to obtain stress deviators either side of cell edges.

Elastoplatic flow capability (2)

- Riemann problem is solved for total stress.
- This corresponds to taking acoustic impedance weighted average for stress deviators.

$$S_{ij}^{*} = \frac{z_1 S_{ij_2} + z_2 S_{ij_1}}{z_1 + z_2}$$

- A full second order approach was found important in solving the nodal momentum equation for elastoplastic flow problems.

Taylor Ta Rod impact problem (1)

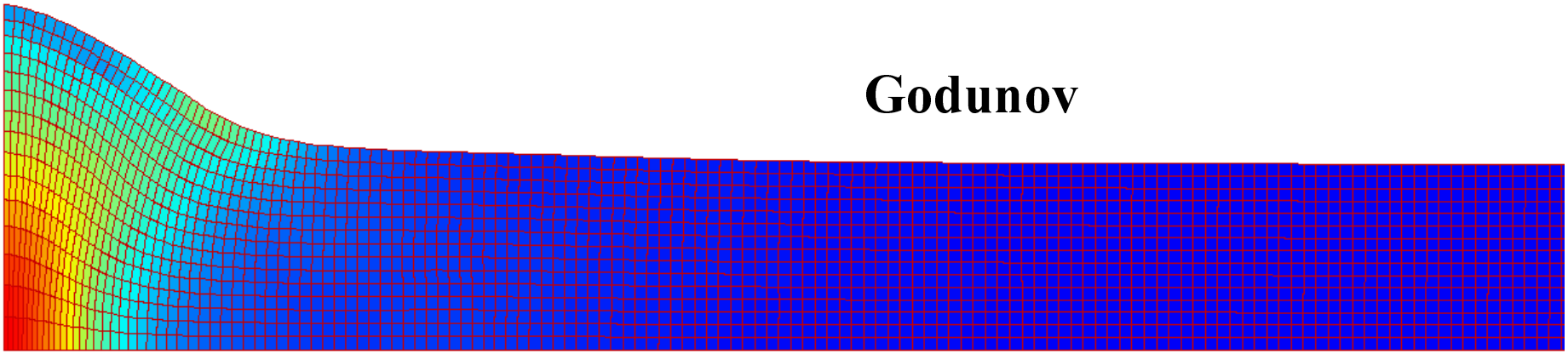

Godunov

Equivalent Plastic Strain at t=40 μs

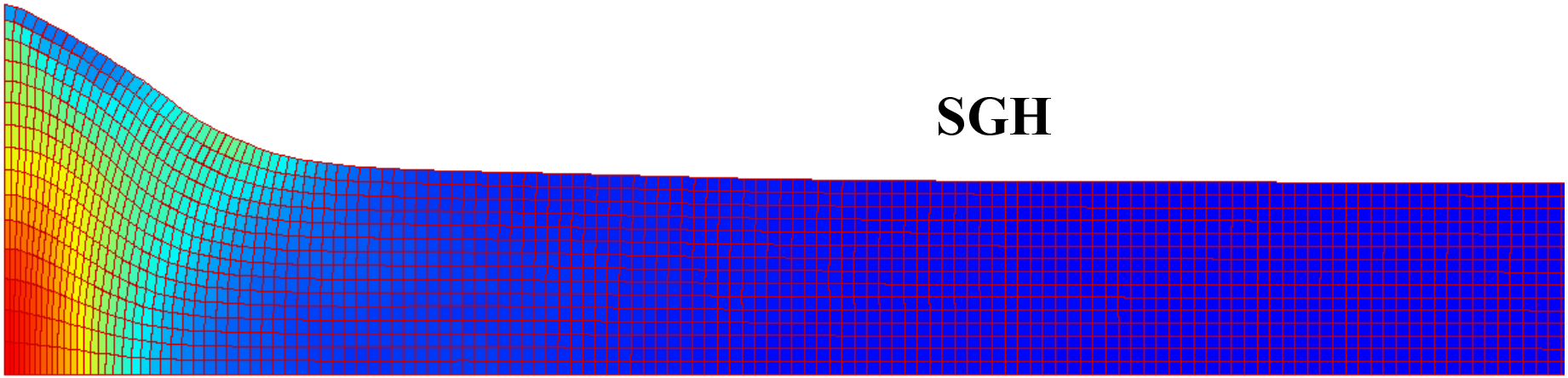

SGH

Taylor Ta Rod impact problem (2)

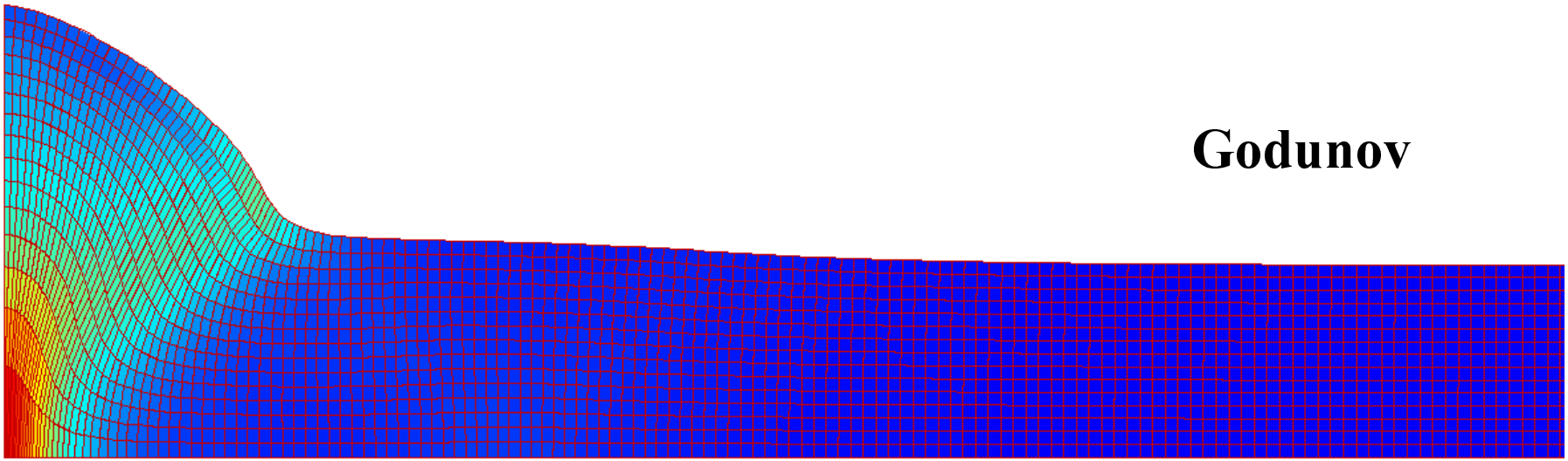

Godunov

Equivalent Plastic Strain at t=80 μs

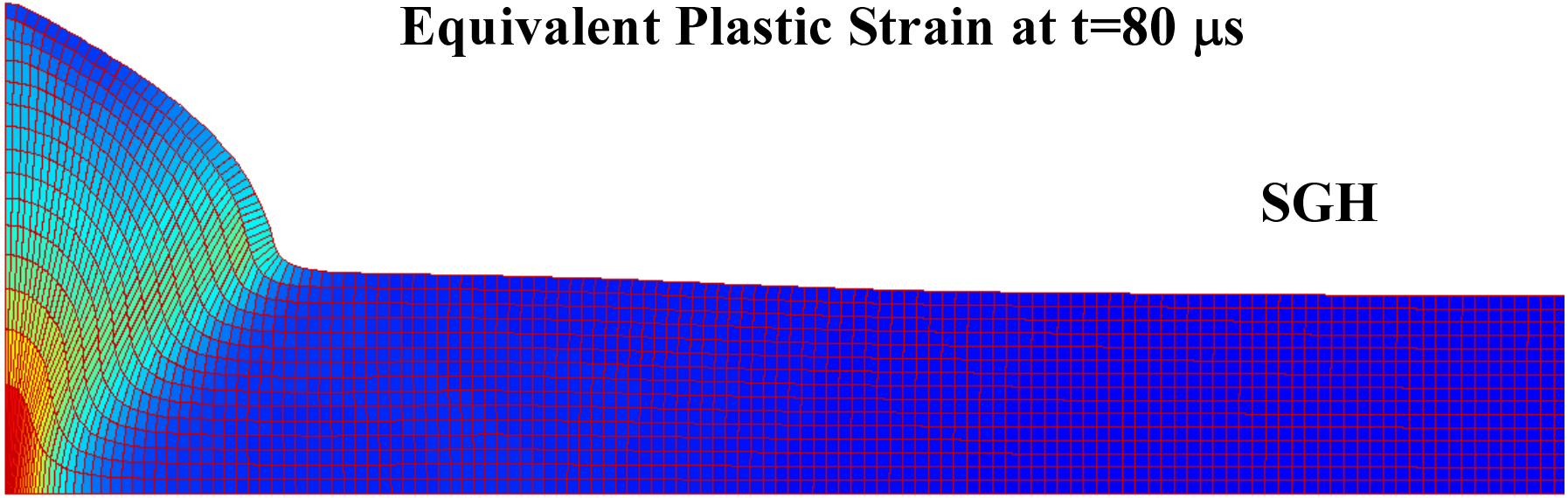

SGH

Taylor Ta Rod impact problem (3)

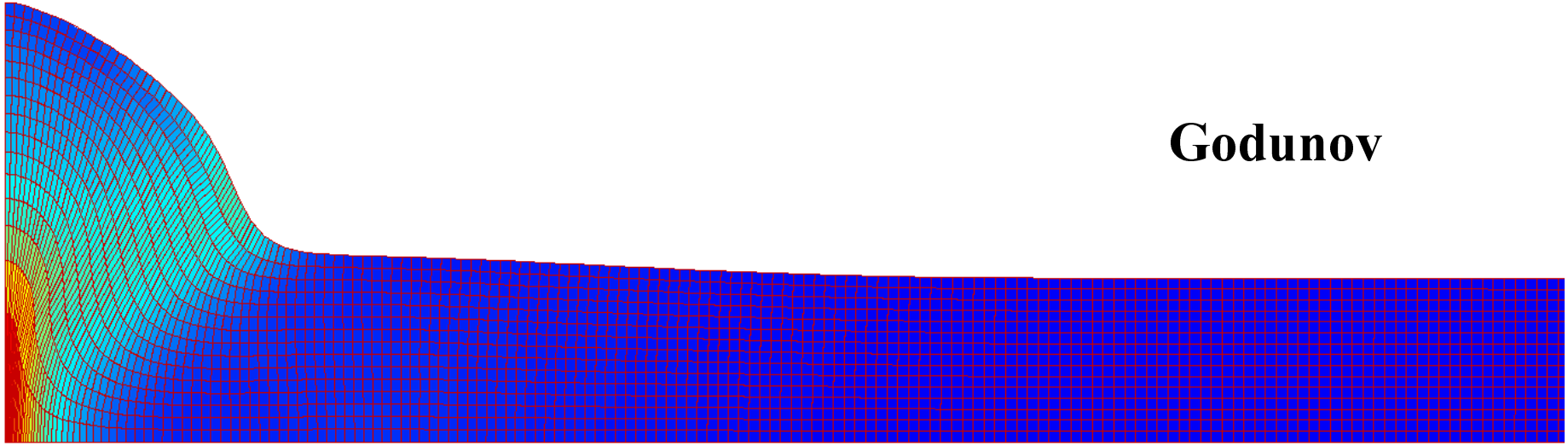

Godunov

Equivalent Plastic Strain at t=120 μs

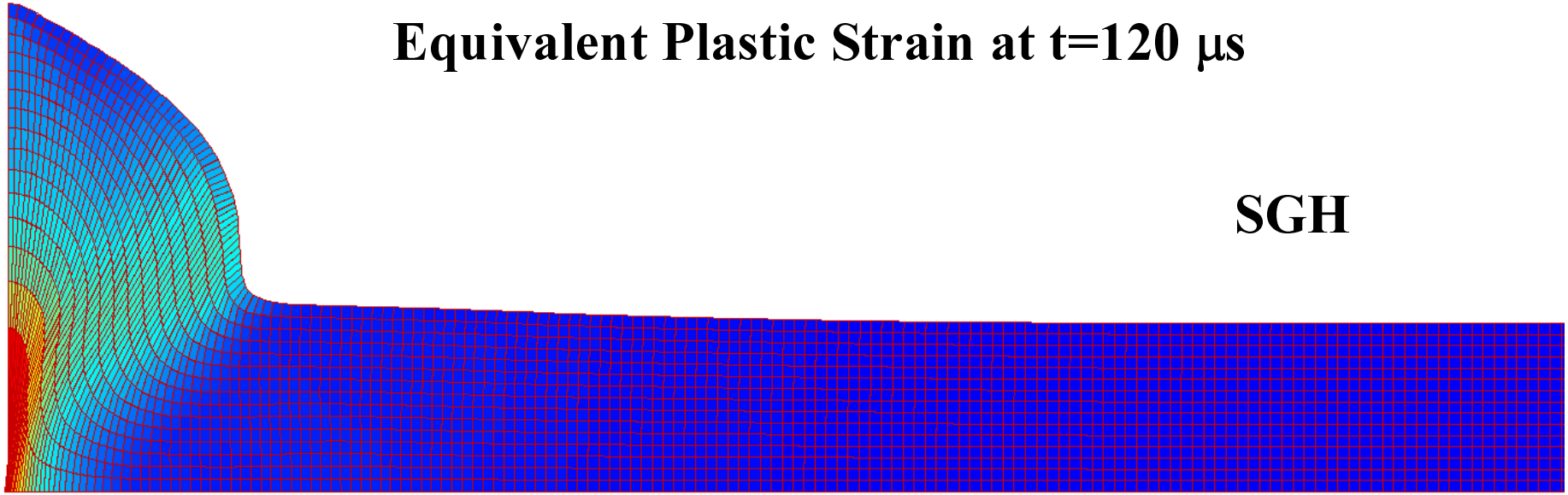

SGH

Conclusion

- A dual grid cell centred Lagrangian Godunov scheme has been extended to 2nd order accuracy in space and time, a cylindrical geometry capability added and preliminary elastoplastic flow capability demonstrated.
- Results have been presented for well known test problems and compared against those obtained with a staggered grid compatible finite element scheme.
- The second order scheme has been shown to retain the benefits observed with the first order scheme in terms of reduced mesh imprinting, symmetry preservation and improved robustness compared to the staggered grid scheme.
- The 2nd order scheme also provides comparable accuracy and shock capturing to staggered grid methods.
- Further improvements in symmetry preservation are observed for cylindrical geometry.
- The elastoplastic flow capability looks promising but needs further work.